SYNTHESIS AND STRUCTURAL ELUCIDATION OF NANOSCALE MANGANESE-BAMBOO COMPOSITES

ISSN: 2141 – 3290
www.wojast.com

SHAIBU, S. E.[1,3]*, INAM[1,3] E. J., MOSES[1] E. A., FATUNLA, O. K.[2,3], ENIN, G. A.[1], OFON, U. A.[2], EFFIONG, N. E. [1]AND IBUOTENANG N. D.[1]

[1]*Department of Chemistry, University of Uyo, Uyo. Nigeria*
[2]*Department of Microbiology, University of Uyo, Uyo. Nigeria*
[3]*International Centre for Energy and Environmental Sustainability Research, University of Uyo, Nigeria*
**Corresponding Author's: shaibusolomon@uniuyo.edu.ng*

ABSTRACT

Owing to the unique features inherent in nanomaterials particularly nanocomposites, enormous attention has been directed at their methods of synthesis, functionalization and modification for broader applications. In this study, chemical and biological methods were employed for the synthesis of nanoscale manganese bamboo composite (nMn-bamboo) with subsequent characterisation. The nanomaterials (nMn and nMn-bamboo) were prepared via aqueous phase borohydride reduction and plant mediated method using curry (*Murrayakoenigii)* leafextracts under ambient conditions. Characterization was done using scanning electron microscopy (SEM), Fourier transform infrared spectroscopy (FTIR), x-ray diffraction (XRD) and particle induced x-ray emission (PIXE) analysis. Significant aggregation and morphological variations were observed among the composites from the SEM micrograph. The XRD analysis revealed the existence of two different manganese oxides peaks in the composites while the FTIR spectra showed the presence of bands at 3441.12 cm^{-1}, 1728.28 cm^{-1}, 1639.55 cm^{-1}, 1604.83 cm^{-1}, 1371.43 cm^{-1} and1332.86 cm^{-1} on the surface of both composites. The nMn-bamboo (plant) had lower concentration of elements (Mn, Al and Si) than nMn-bamboo (chemical) whereas the elements detected in significant concentrations were Mn, Al, Si, and Cl.

INTRODUCTION

Natural nanoparticles are as old as the earth. They have been present for a long time and utilized for different purposes without the full understanding and appreciation of its inherent properties (EPA, 2007). However, nanoparticles (NP) have recently attracted a lot of attention because of wide variety of features and applications in different spheres of life. In the light of its potentials, there has been a sustained worldwide increase in investment in nanotechnology research and development (Nowack*et al*., 2007). Materials in the nanometer range have enjoyed widespread applications in different spheres as a result of their diversity, morphology and chemistry which includes water treatment (Teow *et al.,* 2019; Vikrant and Kim, 2019), metal ion reutilization (Deng *et al.,* 2019) plant disease diagnosis and management (Khan *et al.,* 2019) stem cell research (Aziz *et al.,* 2019; Pacheco-Torgal, 2019), construction (Dahlan *et al.,* 2019), including catalysis (Zhu *et al.,* 2019).

Currently, there are different routes for the synthesis of different types of metal nanoparticles with diverse morphological and chemical characteristics (Ramezani *et al.*, 2019). However, there is an increasing demand for environmentally friendly, economical and safe preparation approaches of metal nanoparticles for societal benefits (Barabadi *et al*., 2017; Ovais *et al.*, 2016). Emerging green nanoparticles are at the leading edge of the nanobiotechnology field. In this regard, the use of biological resources like plants (Maham and Karami-Osboo, 2017) and algae (Dahoumane *et al*., 2017) and microorganisms including bacteria (Amin *et al.*, 2019; Saravanan et al., 2018), actinomycetes (Ovais *et al.*, 2016), yeasts (Niknejad *et al.*, 2015) and fungi (Barabadi and Honary, 2016; 2014; Niknejad *et al.*, 2015). According to the proposition that various biological moieties affect the biogenesis synthesis of metal nanoparticles, hence,

exploring potent and viable innocuous alternatives for preparation of metal nanoparticles has become an area of momentous interest (Barabadi *et al*., 2017; Ovais *et al.*, 2016).

However, its synthesis and applications are sometimes hindered by agglomeration that negatively affects efficiency (Phenrat *et al.,* 2007; O'Carroll *et al.,* 2013). The use of filters, stabilizing agents or support during the synthesis of these nanoparticles help reduce the rate of oxidation (Liu *et al.,* 2014; Bhowmick *et al.,* 2014; Yuan *et al.,* 2009; Kim *et al.,* 2013; Dorathi *et al.,* 2012; Ghosh and Bhattacharyya, 2002; Srinivasan *et al.,* 2011). Eco friendly method of synthesis is globally advocated as complement or alternative to contemporary techniques if economical and robust. This prompted the use of *Murrayakoenigii* leaf extracts and also bamboo for the synthesis of manganese nano composite (Teimuri-Mofad *et al*., 2011). These plant materials are in relatively high abundance in Nigeria and of little economic value. The aim of this study is to synthesize nanoscale manganese-bamboo composites (nMn-bamboo) using borohydride reduction method and plant mediated route in order to evaluate structural and morphological features of the nanocomposites.

EXPERIMENTAL: CHEMICALS AND REAGENTS

Analytical grade Manganese chloride (Kermel, minimum assay 99.9%), sodium borohydride (BDH 95%, prd no. 30114), methylene blue (BDH prd no. 340484B), absolute ethanol (BDH Analar, 95% UN No. 1097), hydrochloric acid (Riedel-deHaen purity 37%, density 1.1kg/cm^3) and sodium hydroxide (BDH prod. No. 30167) were used without further purification. Other basic laboratory glass-wares and apparatus were also used in the course of this research.

MATERIALS AND METHODS

INSTRUMENTATION

The scanning electron micrograph of bamboo, nMn and nMn-bamboo composite was viewed under a FEI^{TM}scanning electron microscope (Nova Nano SEM 230). A 1.7MV tandem pelletron accelerator (model 5SDH) was used to analyze for the concentration of the elements present. X-ray diffraction (XRD) patterns of the nanomaterials were performed on a Rigaku (D/MAX-3B) diffractometer with Cu K_α radiation (λ = 1.54056 A$^\circ$) and a graphite monochromator at 40kV, 30 mA. Fourier transform infrared spectroscopy (FTIR) absorption spectra were obtained using the potassium bromide (KBr) pellet method and the spectra of the samples were recorded over the range 4000 –400 cm^{-1} using Shimadzu (8400s).

PLANT COLLECTION AND PREPARATION

The *Murrayakoenigii* leaves were collected from the vicinity of University of Uyo and the plant was identified by and authenticated in the Department of Botany, botany department University of Uyo while the bamboo stem was sourced from the vicinity of University of Uyo. The *Murrayakoenigii* leaves were thoroughly washed, dried at room temperature for 48 hrs and chopped into small pieces. The extract was prepared by boiling a 10 g of *Murrayakoenigii* for 10 min and the resulting broth was stored at 4 ^{0}C prior to utilization for synthesis. The bamboo stem on the other hand was also carefully washed, chopped and pulverized into very fine bits with the help of mortar and pestle. It was subsequently soaked in HCl solution for 4 hrs, washed several times with deionized water and finally dried at room temperature (Teimuri-Mofad *et al*., 2011).

PREPARATION OF NANOSCALE MANGANESE COMPOSITE (nMn-bamboo)

a). Chemical route

The nanocomposite (nMn-bamboo) was prepared according to a previously reported procedure described method in the literature (Shaibu *et al*., 2014). The nMn-bamboo composite was prepared with $MnCl_2.4H_2O$ and bamboo in the ratio 1:1. A solution of 0.05 M $MnCl_2.4H_2O$ was prepared followed by the addition of 1 g powder of the treated bamboo powder in a beaker. The mixture was and stirred on a magnetic stirrer (model: J. W. Towers) for 2 hours to ensure that the materials were properly mixed. thorough mixture of both materials the resulting solution

was and then transferred into a three-neck flask before the addition of the 0.1 M borohydride solution. After the complete addition of the borohydride solution, the mixture was further stirred for another 30 min (Yuvakkumar*et al.*, 2011).

b) Biological route

Precisely, 50 mL of the extract of *Murrayakoenigii* leaves was added to 50 mL of 1 M $MnCl_2.4H_2O$ solution and 1 g of bamboo powder for *in-situ* reduction of Mn^{2+} ions. The resulting suspension was subsequently centrifuged at 10,000 rpm for 15 minand dried in an oven at 50 ^{0}C before characterization. Additionally, a solution of 1:1 of bamboo powder and $MnCl_2.4H_2O$ was prepared and stirred for 2 hours before the addition of 100 mL of the extract. This was allowed to stand for 24 hours before centrifugation and drying (Teimuri-Mofad *et al*., 2011; Song & Kim 2009).

RESULTS AND DISCUSSION

SCANNING ELECTRON MICROSCOPY (SEM)

Figure 1 presents the image of baboo and nMn-bamboo from the scanning electron microscope. It was observed that the synthesized composites (nMn-bamboo) have changed in its morphology. This change, however, was minimal. This is similar to the observation of The SEM images of bamboo and the synthesized nMn-bamboo composites are presented in Fig. 1.0 and a slightly different morphological feature is evident in the composite (Celebi*et al*., 2007. Observation from Fig. 1.0 reveals that there may be aggregation of the synthesized nanomaterials is as a result of the large surface area, magnetic dipole-dipole interactions and synthesis at ambient conditions of the nanoparticles (Li *et al*., 2006; Phenrat *et al*., 2007). Figure 1c shows the chemically prepared nMn-bamboo (chemical) in Fig. 1.0c shows a bamboo It can be observed that the fibre was completely submerged by nMn particles. In the case of the biological processed nanocomposite, nMn-bamboo, (plant), the surface of the bamboo fibre can be seen to be highly characterized with numerous pores and crevices due to the deposition of the nanoparticles.

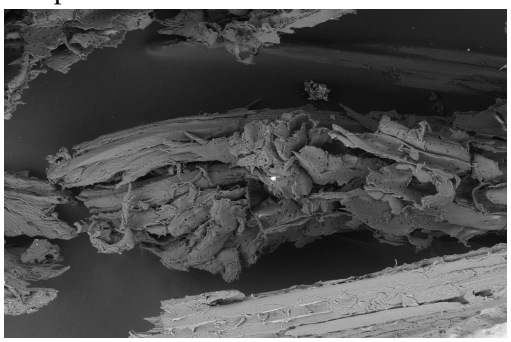

a. Bamboo

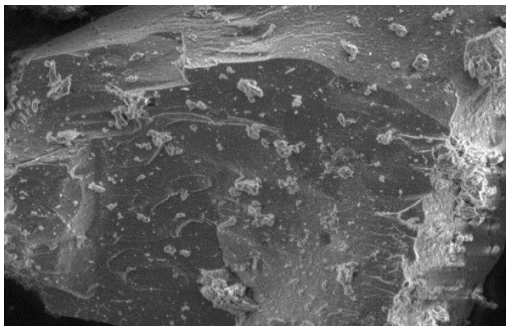

b. nMn (chemical)

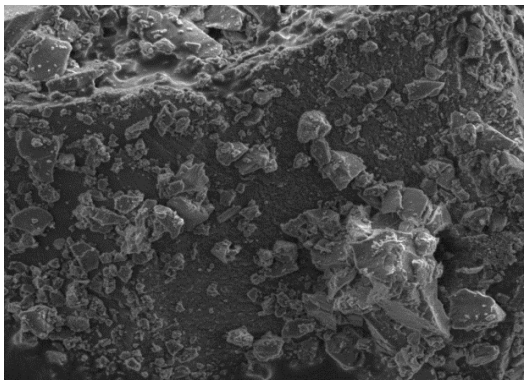

d. nMn-Bamboo (chemical)

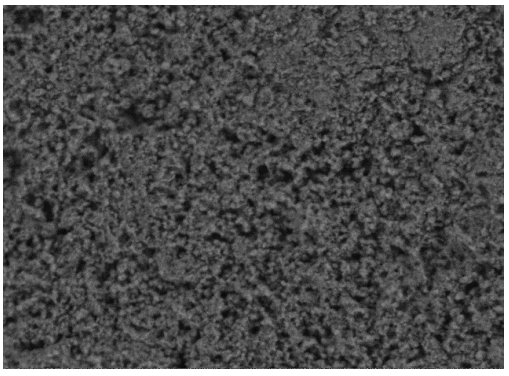

e. nMn-Bamboo (plant)

Figure 1.0: SEM of bamboo, nMn and nMn-bamboo

PARTICLE INDUCED X-ray EMISSION (PIXE)

Table 1 presents the elemental composition of different elements in the samples. The elements present are shown in table 1.0 below and included Al, Si, Cl, K, Ti, Mn, Fe and Ni in different levels of concentrations. The concentration of Mn in the composite synthesized via chemical route was higher in comparison to using plant extracts. And the plant mediated nMn-bamboo reveals systematic decrease in most of the elements(Al, Si, Cl, K, Ti and Mn) compared to the nMn-bamboo (chemical) which could be attributed to the higher reduction ability of $NaBH_4$ than the mild action of the metabolites present in *Murrayakoenigii* extract (Agaja and Obiajunwa, 2012). Evidently, concentrations of the Fe, Zn and Ni in the nMn-bamboo (plant) were significant owing to the inherent presence of these metals in the biological make up of *Murrayakoenigii*. Importantly, the number of elements in the composites (chemical and plant) is not directly proportional to that of its individual constituents (bamboo and nMn) as can be seen from Table 1.0.

Table 1.0: Concentration of elements in bamboo, nMn and nMn-bamboo (chemical and plant) by PIXE analysis

Elements	Bamboo	nMn-Bamboo (Chemical Route)	nMn-Bamboo (Plant Route)
	5116.6	7369.7	6769.4
Si	3116.1	3485.9	2315.9
Cl	301.9	46723.5	24623.2
K	95.4	62.6	12.7
Ca	95.6	445.4	423.1
Ti	11.6	35.4	15.6
Cr	18.5	-	-
Mn	45.1	107411.1	89879.9
Fe	355.8	4121.6	5139.7
Ni	-	56.7	118.6
Zn	8.9	73.4	101.2

- represent below detection level

X-RAY DIFFRACTION

The XRD patterns confirm the presence of combination of two oxides of manganese, Mn_3O_4 and MnOin the nanomaterials. This may be as a result of rapid oxidation of the outer shell of the Mn core. The chemical synthesized nMn and nMn-Bamboo showed higher crystallinity compared to the plant synthesized composites. Peaks (A), (B), and (C), (D), (E) are indicative of the presence of tetragonal Mn_3O_4 and cubic MnO crystalline phases respectively depicted in Figure 2. The diffraction peaks appear at 2Ɵ values of 18.5^0, 24.01^0, 33.89^0, 47.82^0 and 57.61^0 indexed to the (112), (121/211), (222), (004) and (161) in that order (Agaja & Obiajunwa, 2012, Wanga *et al*., 2011 and Wang & Li, 2003). The patterns of the nanocomposites correspond to tetragonal Mn_3O_4 (JCPDS No. 24-0734) and cubic MnO (JCPDS 07-0230).

Fourier Transform Infra Red Spectroscopy (FTIR)

FTIR spectra of bamboo (Fig. 1.1a), shows a strong broad O–H stretching absorption around 3417.98 cm^{-1} and a prominent C–H stretching absorption at about 2939.61 cm^{-1}. C-O stretch was found at 1051.24 cm^{-1}, the non-conjugated C=O stretch (in hemicellulose) was observed at 1728.28 cm^{-1}, and the aromatic skeletal vibration in lignin appeared at 1512.24 cm^{-1} and 1604.83 cm^{-1}. There was also a stronger carbonyl band at 1728.28 cm^{-1}, indicating relatively high-xylan content present in bamboo. This features in bamboo play a vital role in the general properties of the composites and due to composition of the nMn with the bamboo in Fig. 1.1 c,

there was a general increase in the intensity and shift of the absorption bands and also the appearance of a peak at 2899.11 cm^{-1} and 1051.24 cm^{-1} that was not originally present in the spectrum of nMn (Fig. 1.1b) (Coates, 2000).

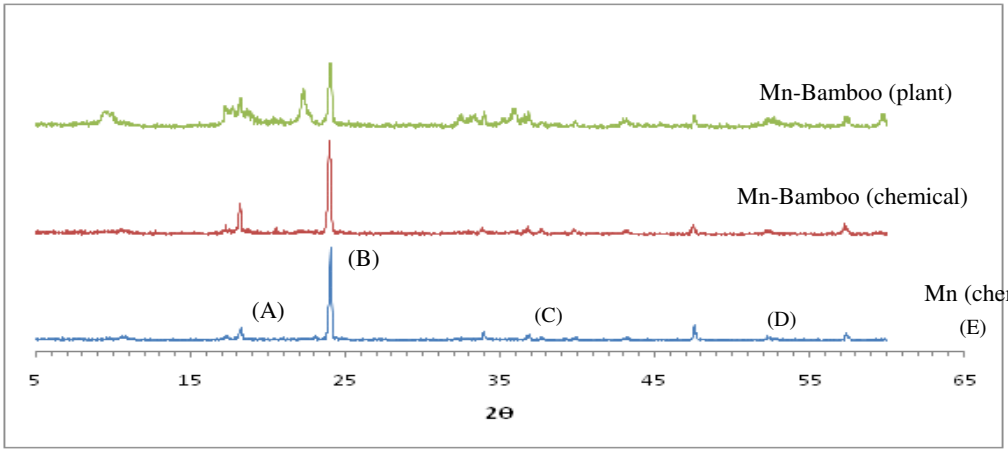

Figure2: XRD patterns of Mn and Mn-Bamboo (chemical) and Mn-Bambo (plant)

Those peaks are attributed to C–H stretching absorption and C-O stretching in the bamboo respectively due to the contribution from the bamboo fibres as shown in spectrum 1.1 a.

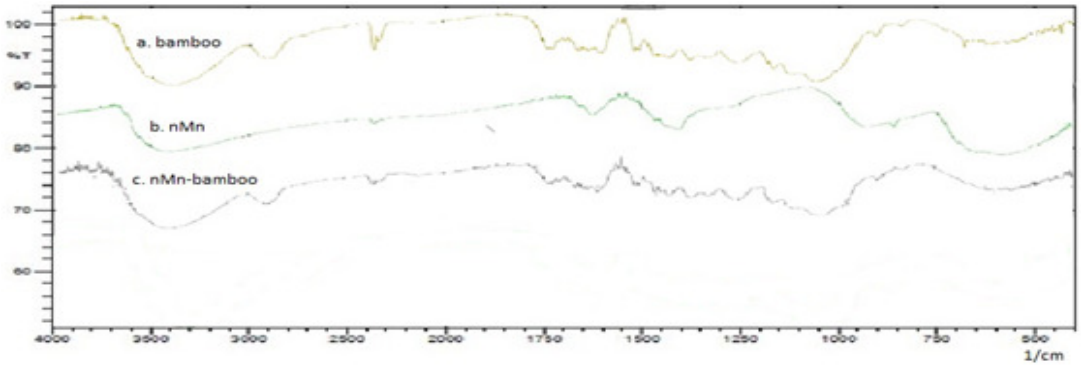

Figure3: FTIR of bamboo, nMn, nMn-bamboo (chemical) and nMn-bamboo (plant)

It is germane to note that the synergistic properties of the composites as a result of the impregnation of nMn into the complex matrix of bamboo will systematically increase its performance in the prospective treatment of a wide variety of contaminants.

CONCLUSION

The elemental composition, phase purity and functional group identification showed that the level of inorganic materials present in the composite materials is a function of the starting materials (nMn and bamboo). The yield of the composites is highly dependent on the strength of the reducing agent. Chemically synthesized showed higher composition of manganese than the plant synthesized manganese nanoparticle. The bamboo filler significantly reduced the rate of agglomeration in the nMn-bamboo as compared to nMn that had no support. However, the presence of negatively charged functional groups on the surface of the composites reflects its suitability as adsorbent for removal of heavy metals and cationic dyes from aqueous media.

The authors declare no conflict of interest

Funding: This work was supported by Tertiary Education Trust Fund (Tetfund) years 2016 – 2018 (merged) Tetfund Research Projects (TRP) Intervention.

REFERENCES

Agaja, S. A., and Obiajunwa, E. I. (2012). Proton–Induced X–Ray Emission (Pixe) analysis of some sea food from Western Niger Delta, Nigeria. *American Journal of Food. Nutr*ition, *2*(2), 51-54.

Amin, Z. R., Khashyarmanesh, Z., Bazzaz, B. S. F. and Noghabi, Z. S. (2019). Does Biosynthetic Silver Nanoparticles Are More Stable with Lower Toxicity than Their Synthetic Counterparts? *Iranian journal of pharmaceutical research,* 18(1): 210-222.

Aziz, S. G. G., Pashaiasl, M., Khodadadi, K. Ocheje, O. (2019). Application of nanomaterials in three□dimensional stem cell culture. *Journal of cellular biochemistry*, 120 (11): 1-9.

Barabadi, H. and Honary, S. (2016). Biofabrication of gold and silver nanoparticles for pharmaceutical applications. *Pharmaceutical and Biomedical Research*, *2*(1): 1-7.

Barabadi, H., Ovais, M., Shinwari, Z. K. and Saravanan, M. (2017). Anti-cancer green bionanomaterials: present status and future prospects. *Green Chemistry Letters and Review*, *10*(4): 285 – 314.

Bhowmick, S., Chakraborty, S., Mondal, P., Van Renterghem, W., Van den Berghe, S., Roman-Ross, G. Iglesias, M. (2014). Montmorillonite-supported nanoscale zero-valent iron for removal of arsenic from aqueous solution: Kinetics and mechanism. *Chemical Engineering Journal*, 243: 14-23.

Celebi O., Uzum C., Shahwan T. and Erten H. N. (2007). Preparation and Characterization of zero-valent iron. *Journal of Hazardous Materials*, 148; 761.

Coates, J. (2000). Interpretation of infrared spectra, a practical approach. *Encyclopedia of analytical chemistry*.

Dahlan, A. S. (2019). Smart and Functional Materials Based Nanomaterials in Construction Styles in Nano-Architecture. *Silicon*, 11(4): 1949-1953.

Dahoumane, S. A., Mechouet, M., Wijesekera, K., Filipe, C. D. M., Sicard, C., Bazylinski, D. A. and Jeffryes, C. (2017). Algae-mediated biosynthesis of inorganic nanomaterials as a promising route in nanobiotechnology – a review.*Green Chemistry*, 19(3): 552 – 587.

Deng, F., Luo, X. B., Ding, L., Luo, S. L. (2019). Application of nanomaterials and nanotechnology in the reutilization of metal ion from wastewater. In *Nanomaterials for the removal of pollutants and resource reutilization* pp. 149-178. Elsevier.

Dorathi, P. J., Kandasamy, P. (2012). Dechlorination of chlorophenols by zero valent iron impregnated silica. *Journal of Environmental Sciences*, 24(4): 765-773.

EPA, Nanotechnology White Paper. U.S. Environmental Protection Agency Report EPA, (2007). 100/B-07/001, Washington DC 20460, USA.

Ghosh, D. Bhattacharyya, K. G. (2002). Adsorption of methylene blue on kaolinite. *Applied Clay Science,* 20(6): 295–300.

Khan, M. R., Rizvi, T. F., Ahamad, F. (2019). Application of Nanomaterials in Plant Disease Diagnosis and Management. *Nanobiotechnology Applications in Plant Protection*, 19-33.

Kim, S. A., Kamala-Kannan, S., Lee, K. J., Park Y. J., Shea, P. J., Lee, W. H., Kim, H. M. Oh, B. T. (2013). Removal of Pb(II) from aqueous solution by a zeolite–nanoscale zero-valent iron composite. *Chemical Engineering Journal*, 217: 54-60.

Li L., Fan M., Brown R.C., van Leeuwen, L. (2006). Synthesis, Properties, and Environmental Applications of Nanoscale Iron-Based Materials: A Review. *Critical Reviews in Environmental Science and Technology,* 36; 405-431.

Liu, T., Wang, Z. L., Yan, X. Zhang, B. (2014). Removal of mercury (II) and chromium (VI) from wastewater using a new and effective composite: Pumice-supported nanoscale zero-valent iron. *Chemical Engineering Journal*, 245: 34-40.

Maham, M. and R. Karami-Osboo (2017). Extraction of Sulfathiazole from Urine Samples Using Biosynthesized Magnetic Nanoparticles.Iranian Journal of Pharmaceutical Research, *16*(2): 462-470.

Niknejad, F., Nabili, M., DaieGhazvini, R. and Moazeni, M. (2015). Green synthesis of silver nanoparticles: Advantages of the yeast *Saccharomyces cerevisiae* model. *Current Medical Mycology*, 1(3): 17-24.

Nowack, Bernd, and Thomas D. Bucheli. (2007). Occurrence, behavior and effects of nanoparticles in the environment." *Environmental pollution* 2007, 150 (1): 5-22.

O'Carroll, D., Sleep, B., Krol, M., Boparai, H. Kocur, C. (2013). Nanoscale zero valent iron and bimetallic particles for contaminated site remediation. *Advances in Water Resources*, 51: 104-122.

Ovais, M., Khalil, A. T., Raza, A., Khan, M. A., Ahmad, I., Islam, N. U. and Shinwari, Z. K. (2016). Green synthesis of silver nanoparticles via plant extracts: beginning a new era in cancer theranostics. *Nanomedicine*, 12(23): 3157-3177.

Pacheco-Torgal, F., (2019). Introduction to nanotechnology in eco-efficient construction. In *Nanotechnology in eco-efficient construction* (pp. 1-9. Woodhead Publishing.

Phenrat, T., Saleh, N., Sirk, K., Tilton, R. D. Lowry, G. V. (2007). Aggregation and sedimentation of aqueous nanoscale zerovalent iron dispersions. *Environmental Science Technology*, *41*(1): 284-290.

Ramezani, T., Nabiuni, M., Baharara, J., Parivar, K., and Namvar, F. (2019). Sensitization of Resistance Ovarian Cancer Cells to Cisplatin by Biogenic Synthesized Silver Nanoparticles Through p53 Activation. *Iranian Journal Pharmaceutical Research*, 18(1):222-231.

Song J. Y. and Kim B. S. (2009). Rapid biological synthesis of silver nanoparticles using plant leaf extracts. *Bioprocess Biosystem Engineering*, 32; 79-88.

Srinivasan, R. (2011). Advances in application of natural clay and its composites in removal of biological, organic, and inorganic contaminants from drinking water. *Advances in Materials Science and Engineering*, 36;*14-24*.

Teimuri-Mofrad R, Hadi R, Tahmasebi B, Farhoudian S, Mehravar M, Nasiri R. (2007). Green synthesis of gold nanoparticles using plant extract: Mini-review. *Nanochemistry Research*, 2(1):8-19.

Teow, Y. H. and Mohammad, A. W. (2019). New generation nanomaterials for water desalination: A review. *Desalination*, 451: 2-17.

Vikrant, K. and Kim, K. H. (2019). Nanomaterials for the adsorptive treatment of Hg (II) ions from water. *Chemical Engineering Journal*, 358: 264-282.

Wang, X. and Li, Y. (2003). Synthesis and Formation Mechanism of Manganese Dioxide Nanowires/Nanorods. *Chemistry European Journal*, 9: 300–306.

Wanga, X., Liua, L., Wanga, X., Yia, L., Hub, C. and Zhanga, X. (2011). Mn_2O_3/carbon aerogel microbead composites synthesized by in situ coating method for supercapacitors. *Materials Science and Engineering B.*, 176, 1232– 1238.

Yuan, P., Fan, M., Yang, D., He, H., Liu, D., Yuan, A. Chen, T. (2009). Montmorillonite-supported magnetite nanoparticles for the removal of hexavalent chromium [Cr (VI)] from aqueous solutions. *Journal of hazardous materials*, *166*(2-3): 821-829.

Yuvakkumar, R., Elango, V., Rajendran, V., Kannan, N. (2011). Preparation and Characterization of Zero-Valent Iron Nanoparticles" Digest Journal of Nanomaterials and biostructures, 6(4); 1771-1776.

Zhang, L. L., Wei, T., Wang, W., and Zhao, X. S. (2009). Manganese oxide–carbon composite as supercapacitor electrode materials. *Microporous and Mesoporous Materials*, *123*(1), 260-267.

Zhu, W., Chen, Z., Pan, Y., Dai, R., Wu, Y., Zhuang, Z. Li, Y., (2019). Functionalization of hollow nanomaterials for catalytic applications: Nanoreactor construction. *Advanced Materials*, *31*(38): 1800426.